Published in final edited form as:
J Comp Neurol. 2014 June 15; 522(9): 2152–2163. doi:10.1002/cne.23523.

Synapses lacking astrocyte appear in the amygdala during consolidation of Pavlovian threat conditioning

Linnaea E. Ostroff[1,*], **Mustfa K. Manzur**[1], **Christopher K. Cain**[1,2], and **Joseph E. LeDoux**[1,2]

[1]Center for Neural Science, New York University, New York, NY

[2]Emotional Brain Institute, Nathan Kline Institute for Psychiatry Research, Orangeburg, NY

Abstract

There is growing evidence that astrocytes, long held to merely provide metabolic support in the adult brain, participate in both synaptic plasticity and learning and memory. Astrocytic processes are sometimes present at the synaptic cleft, suggesting that they might act directly at individual synapses. Associative learning induces synaptic plasticity and morphological changes at synapses in the lateral amygdala (LA). To determine whether astrocytic contacts are involved in these changes, we examined LA synapses after either threat conditioning (also called fear conditioning) or conditioned inhibition in adult rats using serial section transmission electron microscopy (ssTEM) reconstructions. There was a transient increase in the density of synapses with no astrocytic contact after threat conditioning, especially on enlarged spines containing both polyribosomes and a spine apparatus. In contrast, synapses with astrocytic contacts were smaller after conditioned inhibition. This suggests that during memory consolidation astrocytic processes are absent if synapses are enlarging but present if they are shrinking. We measured the perimeter of each synapse and its degree of astrocyte coverage, and found that only about 20–30% of each synapse was ensheathed. The amount of synapse perimeter surrounded by astrocyte did not scale with synapse size, giving large synapses a disproportionately long astrocyte-free perimeter and resulting in a net increase in astrocyte-free perimeter after threat conditioning. Thus astrocytic processes do not mechanically isolate LA synapses, but may instead interact through local signaling, possibly via cell-surface receptors. Our results suggest that contact with astrocytic processes opposes synapse growth during memory consolidation.

Keywords

dendritic spine; postsynaptic density; lateral amygdala; spine apparatus; electron microscopy; synaptic cleft; tripartite synapse; fear conditioning; conditioned inhibition; safety conditioning

Introduction

Astrocytes have long been known to have a crucial role in maintaining the metabolic and ionic environment of the neuropil in the mature brain, and there is now substantial evidence

[*]Corresponding author: Address: 4 Washington Place, Room 809, New York, NY 10003. Phone: 212-998-3945. Fax: 212-995-4704. lostroff@nyu.edu..

Conflict of interest statement The authors have no conflicts to disclose.

that they participate directly in regulating synapse function and synaptic plasticity (Perea et al., 2009; Todd et al., 2006; Allen and Barres, 2005; Wang and Bordey, 2008; Kimelberg, 2010; Theodosis et al., 2008; Pannasch and Rouach, 2013). Synaptic plasticity is believed to underlie learning and memory, and it is easy to imagine astrocytes having a key role here as well. Indeed, several studies have shown that metabolic support from astrocytes is necessary for memory formation, as is release of signaling molecules via the astrocytic connexin subunits Cx-43 and Cx-30 (Stehberg et al., 2012; Lutz et al., 2009; Gibbs et al., 2008; Newman et al., 2011; Suzuki et al., 2011). Exactly how astrocytes exert their influence on synapses is not well understood, but their unique spatial relationship with neurons and their large complement of neurotransmitter receptors and signaling molecules offer a variety of possibilities.

Forebrain astrocytes extend protoplasmic processes throughout the neuropil, forming an elaborate latticework surrounding the axons, dendrites, and neural cell bodies. The tripartite synapse, which includes an astrocytic process at the synaptic cleft, has replaced the traditional concept of a synapse as a contact between two neurons (Reichenbach et al., 2010; Perea et al., 2009). As interest in the role of this third synaptic partner has grown, the fact that astrocytic interactions with synapses are variable and dynamic has been overlooked. In some brain areas astrocytes do not contact synapses directly at all, and in other areas they may not contact every synapse. In addition, astrocytic processes may envelop nearly the entire synaptic cleft or may only touch a small fraction of it. For example, all synapses onto Purkinje cell dendrites are contacted by glial processes, and they ensheath an average of 87% and 65% of the perimeter of climbing fiber and parallel fiber synapses respectively (Xu-Friedman et al., 2001; Spacek, 1985 a). In contrast, only about 60% of synapses in hippocampal area CA1 are contacted by astrocytes, and less than half of their perimeter is surrounded; these values are slightly higher in barrel cortex (Witcher et al., 2007; Ventura and Harris, 1999; Genoud et al., 2006).

Astrocytic processes are quite motile in the neuropil, suggesting that they can rearrange the extent and organization of their synaptic contacts (Haber et al., 2006; Nishida and Okabe, 2007). Indeed, changes in the proportion of synapses with astrocytic contacts and the extent of coverage have been observed in barrel cortex in response to whisker stimulation, in CA1 during recovery after acute slice preparation, and in the hypothalamus in response to hormonal fluctuations (Witcher et al., 2007; Oliet et al., 2008; Genoud et al., 2006). In brain areas where contacts between synapses and astrocytic processes are variable, these contacts could reflect the functional state or recent history of an individual synapse. The synaptic changes that underlie memory are assumed to be specific to a relevant subpopulation of synapses, and contacts with astrocytic processes could potentially contribute to synapse specificity. We therefore investigated the association between astrocytic processes and synapses in an associative learning paradigm.

Pavlovian threat conditioning, also known as fear conditioning (see (LeDoux, 2012) for discussion of terminology) is a simple, robust behavior paradigm in which an animal learns to associate a previously neutral stimulus (often an auditory tone) with an aversive stimulus (usually a mild footshock). Increased excitatory synaptic strength in the lateral amygdala (LA) appears to underlie this associative memory (LeDoux, 2000; Maren, 2005; Sah et al.,

2008). Decreased synapse strength in the LA occurs with conditioned inhibition, a related procedure in which the tone is associated with safety rather than threat (Rogan et al., 2005). Structural plasticity at synapses is thought to be a mechanism of memory storage, and we have shown through ultrastructural measurements that adult rat LA synapses enlarge or shrink during consolidation of threat conditioning and conditioned inhibition, respectively (Kasai and Fukuda, 2010; Bourne and Harris, 2007; Ostroff et al., 2010). Here we have used serial section transmission electron microscopy (ssTEM) to quantify the structure and distribution pattern of astrocytic contacts in the adult rat lateral amygdala (LA) after threat conditioning or conditioned inhibition. Our results indicate that astrocytic contacts are not randomly distributed under either control or learning conditions, and that they are involved in structural changes associated with learning.

Materials and Methods

Analyses were performed on existing serial electron micrographs from previous studies (Ostroff et al., 2010, 2012). All procedures were approved by New York University's Animal Care and Use Committee.

Subjects and behavior

Complete details of behavioral methods and controls have been published elsewhere (Ostroff et al., 2010, 2012). Briefly, adult male rats (n=3 per group) were habituated for 30 minutes to standard conditioning chambers on two consecutive days, then trained on the third day with five presentations of a 30s, 80dB, 5kHz tone and five presentations of a 1s, 0.7mA scrambled footshock in a 32.5 minute training session. For the threat conditioned (TC) group all tones coterminated with shocks, such that the animals learned a threat association to the tone. For the conditioned inhibition (CI) group the tones and shocks were explicitly unpaired such that the animals learned a safety association to the tone. A third group of rats was exposed only to the conditioning chamber and was naïve to the tones and shocks.

Tissue preparation

Detailed sample preparation methods are published elsewhere (Harris et al., 2006, Ostroff et al., 2010). One hour after the first shock during training (or equivalent time for the naïve group) rats were anesthetized with chloral hydrate and perfused with heparinized saline followed by 2.5% glutaraldehyde and 2% paraformaldehyde in 0.1M phosphate buffer (pH 7.4). The brains were removed and immersed in the perfusion fixative for ~2h at room temperature, then rinsed with phosphate buffered saline and sectioned 70 μm on a vibrating slicer (Leica). Tissue sections containing the left LA were processed for electron microscopy. Sections were postfixed for 1h in ferrocyanide-reduced osmium (1.5% potassium ferrocyanide/1% osmium tetroxide) in 0.1M phosphate buffer followed by 1h in 1% osmium tetroxide in 0.1M phosphate buffer, then dehydrated in an ascending series of ethanol containing 1.5% uranyl acetate, infiltrated with LX-112 epoxy resin in descending acetone concentrations, and cured at 60°. Resin was obtained from Ladd Research; all other chemicals were obtained from Electron Microscopy Sciences. Serial sections (range 120–160 sections, mean 143) with even section thickness were cut on an ultramicrotome (Leica)

at 45nm and stained with 1% aqueous uranyl acetate and lead citrate. Images were taken on film at 7500X on a JEOL 1200EX transmission electron microscope, and negatives were digitized using a flatbed scanner (Epson).

A second cohort of rats (n=3 per group) was given identical handling and training as the first cohort, then perfused 24 hours after training. Processing and analysis procedures were the same in both cohorts, except that the 24 hour cohort was perfused with cacodylate buffer instead of phosphate buffer and images were acquired on a JEOL 1230 electron microscope at 7500× magnification with a Gatan Ultrascan 4000 digital camera.

Reconstruction and analysis

Reconstruct software was used for all reconstructions and measurements (Fiala, 2005), and images of three dimensional reconstructions were rendered in 3DS Max (Autodesk). All analysis was done with the experimenters blind to training group.

Series of digital images were aligned and actual section thickness for each series was determined using the cylindrical diameters method (Fiala and Harris, 2001). Segments of spiny dendrites that were in cross section and passed through the central section of each series were reconstructed, including all of their spines and synapses. The length of each dendritic segment was measured as the distance between the first spine contained within the volume on an arbitrarily chosen inclusion end and the last spine on the exclusion end. Spine frequencies were calculated by dividing the count of the spine type in question by the inclusion length, excluding the final spine that defined the dendrite's exclusion end. Synapse size was considered as the two-dimensional area of the post-synaptic density. This was measured directly for oblique orientations, and by multiplying the length of the postsynaptic density on each section by the section thickness for cross sectioned orientations. Synapses were classified as either asymmetric (presumably glutamatergic) or symmetric (presumably GABAergic or modulatory) according to standard morphological criteria (Gray, 1959). A total of 1021 asymmetric spine synapses and 216 (136 asymmetric and 80 symmetric) shaft synapses over 69 spiny dendritic segments from a previous study were analyzed with respect to their astrocytic contacts (Ostroff et al., 2010). For analysis of axons, 136 axon segments with a total of 323 boutons and 217 multiple-synapse boutons from another study were used (Ostroff et al., 2012). In addition, 50 asymmetric and 36 symmetric synapses onto dendritic shafts were randomly chosen.

Statistics

ANOVAs followed by either the Fisher LSD (for training groups) or Bonferroni (for all others) tests were used to compare group means. Bar graphs show means ± standard error of the mean. Hierarchical ANOVAs with rat nested into training group were used to account for individual animals. For effects of training, p values are only reported for significant differences between the naïve group and the TC or CI group. In instances where it is stated that a measure was not changed between groups or for analyses in which multiple groups were collapsed, a factorial ANOVA was used to ensure that there were no significant interactions between groups and independent variables. Correlations are simple regression and R^2 is reported for $p<0.05$.

Results

Increased density of astrocyte-free synapses with threat conditioning

Astrocytic processes were identified by their distinctive morphology (Peters et al., 1991; Reichenbach et al., 2010; Spacek, 1985 a; Ventura and Harris, 1999; Witcher et al., 2007). Astrocytes extend thin, sheetlike processes which intercalate between axons and dendrites in the neuropil, taking on amorphous shapes that conform to the spaces between the more autonomously structured axons and dendrites. This architecture is evident on single sections (Figure 1A–D) and unmistakable in serial reconstructions (Figure 1E). While microglia also extend processes into the neuropil, the two types of glia are easily distinguished. Astrocytes have clear cytoplasm relative to microglia, and contain clusters of filaments and copious glycogen granules (Figure 1A), neither of which are found in microglia.

At some synapses there is direct contact between an astrocytic process and the synaptic cleft (Figure 1A–D, F). To determine how often these contacts occur in the synapse population, we examined the entire perimeter of each synapse for an astrocytic contact. A synapse was considered to have an astrocytic contact if the membrane of astrocytic process was found within 20nm of the synaptic cleft at any point along the synapse perimeter. We found astrocytic contacts at 45 ± 3.3% of asymmetric synapses on dendritic spines in the naïve group, which is somewhat lower than the approximately 60% seen in the adult hippocampus (Ventura and Harris, 1999; Witcher et al., 2007) A significantly lower percentage of synapses had astrocytic contacts in the TC group (34 ± 3.1%, $p<0.01$) but the CI group was not different from the naive. The presence of astrocytic contacts is therefore not random under all conditions; if every synapse were equally likely to have one there would have been no difference between the groups.

To determine whether the training groups differed in absolute synapse numbers, we compared the density of spine synapses per length of dendrite. We did not find a lower density of astrocytic contacts in the TC group, but rather a greater density of synapses lacking astrocytic contacts (Figure 2A). A possible explanation is that all dendrites support a constant baseline number of astrocytic contacts regardless of spine density. If this were true, the percentage of spines with astrocytic contacts should decrease as total spine density increases. However, there was no correlation between spine density and the fraction of synapses with astrocytic contacts (Figure 2B), and a positive correlation between spine density and the density of astrocytic contacts in all training groups (overall $R^2=0.6$, $p<0.0001$). It is possible that some segments of dendrite are more likely than others to have astrocytic contacts. If this were the case, there would be an inverse correlation between synapses with and without astrocyte. In fact, there is a weak but significant positive correlation in the TC group only (Figure 2C). Overall, these data indicate that the likelihood of an astrocytic contact at an individual synapse is neither random nor regulated by the parent dendrite.

Astrocytic contacts at different morphological spine types

Interactions with astrocytes can influence spine morphology in adult animals, and astrocytes are involved in spine and synapse maturation in immature preparations (Christopherson et

al., 2005; Murai et al., 2003; Nishida and Okabe, 2007; Ullian et al., 2004). Time-lapse imaging in adult cortex indicates that spines with enlarged heads are mature and stable over time (Grutzendler et al., 2002; Holtmaat et al., 2006). We sorted LA spines into two morphological categories with respect to the presence of the spine apparatus, a membranous organelle with an undefined role in synaptic plasticity (Figure 1B–D; Jedlicka et al., 2008; Spacek, 1985 b). Spines containing a spine apparatus (SA) are six times larger than spines lacking a spine apparatus (SA-free), and appear more frequently in the TC group (Ostroff et al., 2010). In the naïve group, 56% of SA spines and 43% of SA-free spines in the LA had astrocytic contacts. The density of both SA-free and SA synapses without astrocytic contacts was higher in the TC group, while the density of astrocytic contacts on both spine types was equal across training groups (Figure D–E).

Consolidation of threat conditioning into long-term memory requires new protein synthesis, and there are more polyribosomes in dendrites and spines after threat conditioning (Schafe and LeDoux, 2000; Ostroff et al., 2010; Maren et al., 2003). This suggests that local protein synthesis is involved in synapse-specific plasticity during learning, and polyribosomes could indicate active synapses (Helmstetter et al., 2008; Sutton and Schuman, 2006). Polyribosomes were identified in dendritic spines as small clusters of at least three 10–25nm dark puncta (Steward and Levy, 1982; Ostroff et al., 2002). We found that the higher density of SA spines without astrocytic contacts in the TC group was specific to spines containing polyribosomes (Figure 2F). There was no effect of polyribosome presence on SA-free spines (data not shown).

Astrocytic contacts do not occur uniformly on axons and boutons

Synapses along a dendrite presumably experience different activity patterns, as they are for the most part contacted by different axons. Boutons along an axon, on the other hand, are all activated together. We have reported previously that 16% of boutons in the LA form synapses with more than one postsynaptic partner (Ostroff et al., 2012); these synapses also should receive identical patterns of action potentials. We examined reconstructed segments of axons and multiple-synapse boutons (MSBs) to determine whether their synapses were uniform in the presence or absence of astrocytic contacts. Along individual axon segments, an average of 45 ± 3% of boutons had astrocytic contacts at their synapses. These were on all of the boutons of 16 ± 4% of axons, and none of the boutons of 25 ± 4%. Among MSBs with two asymmetric synapses, 14 ± 2 had astrocytic contacts at both synapses, 42 ± 3% at one, and 45 ± 4% at neither. Thus, like dendrites, the presence of an astrocytic contact is specific to the synapse and not its parent process. There were no differences between training groups in any of these measures.

Astrocytic processes do not proportionally cover the synapse perimeter

Astrocytes take up glutamate through transporters, and processes in direct contact with synapses are in a position to regulate both glutamate kinetics in the synaptic cleft and spillover of glutamate into the neuropil (Anderson and Swanson, 2000; Huang and Bergles, 2004). The amount of glutamate spillover at synapses depends, at least in part, on how much of the synapse is surrounded by astrocyte (Nedergaard and Verkhratsky, 2012). To determine whether LA synapses are substantially ensheathed by astrocytic processes and

whether this is affected by learning, we measured the total perimeter length of each synaptic cleft and the perimeter length that was covered by astrocyte. To obtain the perimeter length, points were placed at the edges of the synaptic cleft on each section and the distance between them was measured, taking the section thickness into account. Points at which an astrocytic process was in contact with the synaptic cleft were used to measure the length of astrocytic contact (Figure 3A–B). The total synapse perimeter was tightly correlated with two-dimensional synapse area over the whole dataset (R^2=0.89). No perimeter measurements varied with training ($p>0.8$), so the groups were collapsed for analysis. Astrocytic contacts were longer on SA synapses than on SA-free synapses, but the fraction of synaptic perimeter covered by astrocyte was higher at SA-free synapses (Figure 3C–D). SA synapses had far greater astrocyte-free perimeter length, regardless of whether any astrocyte was present, while SA-free synapses had significantly more astrocyte-free perimeter when there was no astrocyte (Figure 3E). The length of astrocyte contact was not correlated with postsynaptic density (PSD) area for either spine type (Figure 3E). These measurements reveal that astrocytic processes surround approximately only 20–30% of the perimeter of LA synapses and the amount they surround is not proportional to synapse size, as has also been reported in the hippocampus (Witcher et al., 2007; Spacek, 1985 a; Ventura and Harris, 1999). The length of the synaptic cleft covered by astrocytic processes is thus relatively constant while the length that is not covered is more variable. This is further evidence that astrocytic contacts are not random, since if astrocytic processes were equally likely to occur everywhere in the neuropil they would have proportionally more contact with larger synapses.

PSD area was equal across training groups on SA-free synapses regardless of astrocytic contacts, while SA synapses with astrocytic contacts were smaller in the CI group. SA synapses with astrocytic contacts were larger than those without in the naïve and TC groups (Figure 3G). Astrocytic processes are known to limit glutamate spillover by ensheathing the synaptic cleft at hypothalamic synapses (Oliet et al., 2008). The length of synapse perimeter that is not covered by astrocytic processes could thus be an index of the potential for gluatamate spillover into the neuropil. To assess whether the training groups differed in the amount of synapse perimeter open to the neuropil, we calculated the total astrocyte-free perimeter length of asymmetric spine synapses per length of dendrite. The normalized amount of open perimeter was greater in the TC group ($p<0.03$), and this difference was due specifically to SA spines (Figure 3H). This is unsurprising, given the greater number of these spines in the TC group.

Astrocytic contacts are present at shaft synapses

Both asymmetric and symmetric synapses occur on dendritic shafts in the LA. We previously found that asymmetric shaft synapses in this dataset are always formed by axons which also make spine synapses; these synapses therefore share activity patterns if not necessarily structure (Ostroff et al., 2012). We found that in the naïve group approximately 30% of asymmetric and 6% of symmetric shaft synapses had astrocytic contacts (Figure 4A). Training affected the two synapse types differently. The density of asymmetric synapses without astrocyte was lower in the TC group, while the density of symmetric synapses with astrocyte was higher in the TC group (Figure 4B–C).

The length of astrocyte-free perimeter was equal at symmetric and asymmetric shaft synapses regardless of whether an astrocytic contact as present, as was the case with SA synapses (Figure 4D). Asymmetric shaft synapses are intermediate in size between SA-free and SA synapses, and accordingly the length of astrocyte-free perimeter at asymmetric shaft synapses is significantly larger than that of SA-free synapses and smaller than that of SA synapses ($p<0.001$). There was no difference between the training groups in the amount of astrocyte-free asymmetric synapse perimeter (Figure 4E). In all of the morphological arrangements that we studied, astrocyte contacts seem to have a relatively constant size that does not scale up substantially with the length of the synapse perimeter. Thus overall, asymmetric synapses with longer perimeters have longer astrocyte-free perimeters (Figure 4E).

The decreased proportion of astrocytic contacts after threat conditioning is transient

Consolidation of short-term memory into long-term memory occurs during the first several hours after training, and the stabilization of synaptic changes is presumed to be actively occurring during this time (Schafe and LeDoux, 2000; Maren et al., 2003; Nader et al., 2000). To determine whether the reduced fraction of synapses with astrocytic contacts persists into the long-term memory phase, we collected tissue 24 hours after training. In contrast to consolidation, the percentage of synapses with astrocytic contacts was not reduced in the TC group (48±−2.4% versus 50±−2.4% in the naïve group). There was accordingly no difference in the density of synapses with astrocytic contacts (Figure 4G). The effects of training on synapse size were also different at this time point. Synapses with astrocytic contacts on spines with a spine apparatus were larger in the TC group, while synapses without astrocytic contacts were larger in the CI group.

Discussion

Astrocytes were originally thought to be support cells, acting to maintain metabolic and ionic homeostasis while neurons did the information processing. It is now evident that astrocytes can modulate synaptic function and plasticity, and thus may participate much more directly in the functions of the brain (Ben Achour and Pascual, 2010; Perea and Araque, 2006, 2005; Barker and Ullian, 2010). Astrocytic processes have enormous surface area and penetrate the neuropil extensively, and could presumably exert many of their effects without making direct physical contact with synapses. Our results show that contacts between astrocytic processes and the synaptic cleft do not occur randomly in the LA, however, which suggests that these contacts are functionally meaningful. By examining synapse-astrocyte contacts in two different learning paradigms at two different time points, we have gained insight into the nature of these contacts and their involvement in memory formation and storage in adult animals. Taken as a whole, our data are consistent with an association between astrocytic contacts and synapse stability in the adult LA.

Imaging of adult cortical spines in vivo has shown that the largest spines are the most stable over time, and a prevailing hypothesis holds that memory is stored by stable, enlarged synapses that maintain enhanced connectivity of relevant networks (Holtmaat et al., 2006; Grutzendler et al., 2002; Bourne and Harris, 2007; Kasai and Fukuda, 2010). Our

observations of more spines with a spine apparatus (the largest spines) during consolidation of threat conditioning and the enlargement of synapses on these spines in the long-term memory phase are in line with this model. We found that enlarged spines in the adult LA had astrocytic contacts during the long-term memory phase, but not the consolidation phase of threat conditioning. Memory consolidation is a period of active synapse remodeling and stabilization, and consolidation of threat conditioning is characterized by a time-limited requirement for new protein synthesis in the LA (Schafe and LeDoux, 2000; Maren et al., 2003; Nader et al., 2000). The increased number of synapses without astrocytic contacts, but with a spine apparatus and polyribosomes, suggests that this process occurs in the absence of astrocytic processes. This appears to be specific to synapse enlargement, as decreased synapse size during consolidation of conditioned inhibition was associated with the presence of astrocytic contacts.

While threat conditioning results in stronger LA synapses and a nearly indelible memory, conditioned inhibition weakens LA synapses and produces an association which is easily reversed (Rogan et al., 2005; Ostroff et al., 2010). There was no net difference in synapse size during the long-term memory phase of conditioned inhibition, so the larger size of synapses with astrocytic contacts in this group was presumably due to a shift of astrocytic processes away from the largest synapses. Thus the largest synapses in the group with a stable memory have astrocytic contacts, while the largest synapses in the group with a more labile memory do not. Live imaging of hippocampal dendrites has shown that direct contact with astrocytic processes is necessary for spine maturation and stabilization, but not initial formation (Nishida and Okabe, 2007). A positive relationship between spine size, stability, and persistent astrocyte contact has also been reported in hippocampal dendrites (Haber et al., 2006). If this is true in the adult LA, our data reflect a lower degree of stability and maturity in the spine population during consolidation of threat conditioning and a higher degree during long-term memory, consistent with current models of memory formation at synapses.

In contrast to the cerebellum, where most of the perimeter of every synapse is ensheathed by glial processes, we found that fewer than half of all LA synapses are contacted by astrocytic processes and that only 20–30% of the synaptic cleft is surrounded. The extent of astrocyte contact did not scale up with synapse size and was not affected by our training protocols, unlike barrel cortex, where whisker stimulation increases the length of covered perimeter (Genoud et al., 2006). Our results are more similar to those of Witcher et al. (2007), who found fewer synapses associated with astrocytic processes in recovering adult hippocampal slices. Like threat conditioning, slice recovery induces synaptogenesis, so it is possible that synaptogenesis and synapse growth specifically occur without astrocyte contact. Also like the LA, the degree of synapse ensheathment in hippocampal slices is incomplete and does not vary with synapse size or between treatment groups (Ventura and Harris, 1999; Witcher et al, 2007).

Glutamate clearance is presumed to be a major reason for the close spatial proximity between astrocytes and synapses. Glutamate spillover in the hypothalamus is inversely related to the degree of synapse ensheathment by astrocytes, and astrocytic glutamate transporter expression rises with the degree of synapse ensheathment in barrel cortex after

whisker stimulation (Panatier and Oliet, 2006; Genoud et al., 2006). Our observations in the LA, along with others' in the hippocampus, suggest that astrocytes in these regions do not regulate glutamate spillover in a synapse specific manner by mechanical ensheathment of individual synapses, but may instead clear glutamate more generally throughout the neuropil. This also implies that larger synapses, having larger open perimeters, have concomitantly greater opportunity to activate neighboring synapses via glutamate spillover.

If astrocytic processes are not acting as mechanical glutamate buffers at the synaptic cleft in the LA, they might engage in precisely localized cell-surface signaling with one or both of the other synaptic partners. The only such interaction that has been identified to date is between ephrin-A3 on astrocytic processes and EphA4 on dendritic spines of the hippocampus. Activation of EphA4 induces spine collapse, while disruption of EphA4 or ephrin-A3 results in disorganized, immature spine morphology. It has been suggested that EphA4 signaling stabilizes enlarged spines by counterbalancing mechanisms favoring further spine enlargement (Carmona et al., 2009; Fu et al., 2007; Murai et al., 2003). Although it is unknown whether LA astrocytes express ephrin-A3, our data would support such a relationship between astrocytic processes and spines. During consolidation, when synapse size is likely to be actively changing, the size of synapses with astrocytic contacts was unchanged with threat conditioning and decreased with conditioned inhibition. This could potentially be due to signaling from astrocytes that prevents or even counteracts synapse enlargement under conditions of plasticity.

One intriguing question that our data cannot address is that of which synapses had astrocytic contacts at the time of training. It is possible that astrocytic processes are expelled from some synapses in response to learning, prior to enlargement. Something like this happens in hippocampal cultures, where glutamate application induces retraction of astrocytic processes from the vicinity of mushroom spine heads. This is followed by extension of protrusions from the spine heads (Verbich et al., 2012). Another possibility is that the presence of an astrocytic process alters synaptic transmission such that activity that would otherwise induce enlargement is dampened. During threat conditioning, small synapses activated in the absence of astrocytic contact might enlarge and acquire a spine apparatus, while astrocytic processes at other synapses prevent the same activity from inducing plasticity. This is consistent with an association between astrocytes and stable synapses; astrocytes could minimize plasticity at a specific subset of synapses, while leaving others free to enlarge.

Our results show that the tripartite synapse arrangement is dynamic under learning conditions, and that the presence or absence of an astrocytic process may reflect the functional state of a synapse. This means that at least some interactions between astrocytes and neurons are highly localized and synapse-specific. It is well accepted that astrocytes regulate ion and nutrient concentrations in the extracellular space, and that they communicate extensively with neurons via a variety of chemical messengers. However, little attention has been paid to the possibility that astrocytes, like neurons, may have polarized subcompartments or microdomains. Furthermore, the likely importance of astrocyte-neuron signaling via cell-surface molecules or extracellular microdomains is largely unexplored. This could be an unappreciated confound in interpreting studies of synapses in neuronal cultures. Neurons are routinely cultured in several different ways with respect to astrocytes,

including plating them directly onto a layer of astrocytes, suspending them above but out of physical contact with astrocytes, and omitting astrocytes entirely from the preparation (Segal et al., 1998; Jones et al., 2012; Kaech and Banker, 2006; Brewer et al., 1993). If astrocytic processes are an intrinsic functional component of individual synapses, there may be fundamental differences between synapses in these culture preparations. As our understanding of the role of astrocytes in synapse function, synaptic plasticity, and memory continues to evolve, we expect that synapse-specific interactions will emerge as fundamental mechanisms.

Acknowledgments

Thanks to Libby Perry for expert serial sectioning and Joseph Bedont for help with some of the analysis.

This work was supported by NIH R01-MH046516 and P50-MH058911 to JEL, NIH F32-MH083583 and R21MH094965 to LEO, and NIH F32-MH077458 to CKC.

Role of authors All authors had full access to all the data in the study and take responsibility for the integrity of the data and the accuracy of the data analysis. Study concept and design: LEO, CKC, and JEL. Acquisition of data: LEO, CKC, and MM. Analysis and interpretation of data: LEO and MM. Drafting of the manuscript: LEO and JEL. Critical revision of the manuscript for important intellectual content: CKC and JEL. Statistical analysis: LEO. Obtained funding: LEO, CKC, and JEL.

Literature Cited

Allen N, Barres B. Signaling between glia and neurons: focus on synaptic plasticity. Curr Opin Neurobiol. 2005; 15:542–8. [PubMed: 16144764]

Anderson CM, Swanson RA. Astrocyte glutamate transport: review of properties, regulation, and physiological functions. Glia. 2000; 32:1–14. [PubMed: 10975906]

Barker AJ, Ullian EM. Astrocytes and synaptic plasticity. The Neuroscientist. 2010; 16:40–50. [PubMed: 20236948]

Ben Achour S, Pascual O. Glia: the many ways to modulate synaptic plasticity. Neurochem Int. 2010; 57:440–5. [PubMed: 20193723]

Bourne J, Harris KM. Do thin spines learn to be mushroom spines that remember? Curr Opin Neurobiol. 2007; 17:381–386. [PubMed: 17498943]

Brewer GJ, Torricelli JR, Evege EK, Price PJ. Optimized survival of hippocampal neurons in B27-supplemented Neurobasal, a new serum-free medium combination. J Neurosci Res. 1993; 35:567–76. [PubMed: 8377226]

Carmona MA, Murai KK, Wang L, Roberts AJ, Pasquale EB. Glial ephrin-A3 regulates hippocampal dendritic spine morphology and glutamate transport. Proc Natl Acad Sci U S A. 2009; 106:12524–9. [PubMed: 19592509]

Christopherson KS, Ullian EM, Stokes CCA, Mullowney CE, Hell JW, Agah A, Lawler J, Mosher DF, Bornstein P, Barres BA. Thrombospondins are astrocyte-secreted proteins that promote CNS synaptogenesis. Cell. 2005; 120:421–33. [PubMed: 15707899]

Deininger K, Eder M, Kramer ER, Zieglgänsberger W, Dodt H-U, Dornmair K, Colicelli J, Klein R. The Rab5 guanylate exchange factor Rin1 regulates endocytosis of the EphA4 receptor in mature excitatory neurons. Proc Natl Acad Sci U S A. 2008; 105:12539–44. [PubMed: 18723684]

Fiala JC, Harris KM. Cylindrical diameters method for calibrating section thickness in serial electron microscopy. J Microsc. 2001; 202:468–472. [PubMed: 11422668]

Fiala JC. Reconstruct: a free editor for serial section microscopy. J Microsc. 2005; 218:52–61. [PubMed: 15817063]

Fu W-Y, Chen Y, Sahin M, Zhao X-S, Shi L, Bikoff JB, Lai K-O, Yung W-H, Fu AKY, Greenberg ME, et al. Cdk5 regulates EphA4-mediated dendritic spine retraction through an ephexin1-dependent mechanism. Nat Neurosci. 2007; 10:67–76. [PubMed: 17143272]

Genoud C, Quairiaux C, Steiner P, Hirling H, Welker E, Knott GW. Plasticity of astrocytic coverage and glutamate transporter expression in adult mouse cortex. PLoS Biol. 2006; 4:e343. [PubMed: 17048987]

Gibbs M, Hutchinson D, Hertz L. Astrocytic involvement in learning and memory consolidation. Neurosci Biobehav Rev. 2008

Gray EG. Electron microscopy of synaptic contacts on dendrite spines of the cerebral cortex. Nature. 1959; 183:1592–1593. [PubMed: 13666826]

Grutzendler J, Kasthuri N, Gan WB. Long-term dendritic spine stability in the adult cortex. Nature. 2002; 420:812–816. [PubMed: 12490949]

Haber M, Zhou L, Murai KK. Cooperative astrocyte and dendritic spine dynamics at hippocampal excitatory synapses. J Neurosci. 2006; 26:8881–91. [PubMed: 16943543]

Harris KM, Perry E, Bourne J, Feinberg M, Ostroff L, Hurlburt J. Uniform serial sectioning for transmission electron microscopy. J Neurosci. 2006; 26:12101–12103. [PubMed: 17122034]

Helmstetter FJ, Parsons RG, Gafford GM. Macromolecular synthesis, distributed synaptic plasticity, and fear conditioning. Neurobiol Learn Mem. 2008; 89:324–337. [PubMed: 17977027]

Holtmaat A, Wilbrecht L, Knott GW, Welker E, Svoboda K. Experience-dependent and cell-type-specific spine growth in the neocortex. Nature. 2006; 441:979–983. [PubMed: 16791195]

Huang YH, Bergles DE. Glutamate transporters bring competition to the synapse. Curr Opin Neurobiol. 2004; 14:346–52. [PubMed: 15194115]

Jedlicka P, Vlachos A, Schwarzacher SW, Deller T. A role for the spine apparatus in LTP and spatial learning. Behav Brain Res. 2008; 192:12–19. [PubMed: 18395274]

Jones EV, Cook D, Murai KK. A neuron-astrocyte co-culture system to investigate astrocyte-secreted factors in mouse neuronal development. Methods Mol Biol. 2012; 814:341–52. [PubMed: 22144317]

Kaech S, Banker G. Culturing hippocampal neurons. Nat Protoc. 2006; 1:2406–15. [PubMed: 17406484]

Kasai H, Fukuda M. Structural dynamics of dendritic spines in memory and cognition. Trends Neurosci. 2010; 33:121–9. [PubMed: 20138375]

Kimelberg H. Functions of mature mammalian astrocytes: a current view. The Neuroscientist. 2010; 16:79–106. [PubMed: 20236950]

LeDoux J. Rethinking the emotional brain. Neuron. 2012; 73:653–76. [PubMed: 22365542]

LeDoux JE. Emotion Circuits in the Brain. Annu Rev Neurosci. 2000; 23:155–184. [PubMed: 10845062]

Lutz SE, Zhao Y, Gulinello M, Lee SC, Raine CS, Brosnan CF. Deletion of astrocyte connexins 43 and 30 leads to a dysmyelinating phenotype and hippocampal CA1 vacuolation. J Neurosci. 2009; 29:7743–52. [PubMed: 19535586]

Maren S, Ferrario CR, Corcoran KA, Desmond TJ, Frey KA. Protein synthesis in the amygdala, but not the auditory thalamus, is required for consolidation of Pavlovian fear conditioning in rats. Eur J Neurosci. 2003; 18:3080–3088. [PubMed: 14656303]

Maren S. Synaptic mechanisms of associative memory in the amygdala. Neuron. 2005; 47:783–786. [PubMed: 16157273]

Murai KK, Nguyen LN, Irie F, Yamaguchi Y, Pasquale EB. Control of hippocampal dendritic spine morphology through ephrin-A3/EphA4 signaling. Nat Neurosci. 2003; 6:153–60. [PubMed: 12496762]

Nader K, Schafe GE, Le Doux JE. Fear memories require protein synthesis in the amygdala for reconsolidation after retrieval. Nature. 2000; 406:722–6. [PubMed: 10963596]

Nedergaard M, Verkhratsky A. Artifact versus reality--how astrocytes contribute to synaptic events. Glia. 2012; 60:1013–23. [PubMed: 22228580]

Newman LA, Korol DL, Gold PE. Lactate produced by glycogenolysis in astrocytes regulates memory processing. PLos One. 2011; 6:e28427. [PubMed: 22180782]

Nishida H, Okabe S. Direct astrocytic contacts regulate local maturation of dendritic spines. J Neurosci. 2007; 27:331–40. [PubMed: 17215394]

Oliet SHR, Panatier A, Piet R, Mothet J-P, Poulain DA, Theodosis DT. Neuron-glia interactions in the rat supraoptic nucleus. Prog Brain Res. 2008; 170:109–17. [PubMed: 18655876]

Ostroff LE, Cain CK, Bedont J, Monfils MH, Ledoux JE. Fear and safety learning differentially affect synapse size and dendritic translation in the lateral amygdala. Proc Natl Acad Sci U S A. 2010; 107:9418–9423. [PubMed: 20439732]

Ostroff LE, Cain CK, Jindal N, Dar N, Ledoux JE. Stability of presynaptic vesicle pools and changes in synapse morphology in the amygdala following fear learning in adult rats. J Comp Neurol. 2012; 520:295–314. [PubMed: 21674493]

Ostroff LE, Fiala JC, Allwardt B, Harris KM. Polyribosomes redistribute from dendritic shafts into spines with enlarged synapses during LTP in developing rat hippocampal slices. Neuron. 2002; 35:535–545. [PubMed: 12165474]

Panatier A, Oliet SHR. Neuron-glia interactions in the hypothalamus. Neuron glia biology. 2006; 2:51–8. [PubMed: 18634590]

Pannasch U, Rouach N. Emerging role for astroglial networks in information processing: from synapse to behavior. Trends Neurosci. 2013; 36:405–17. [PubMed: 23659852]

Perea G, Araque A. Properties of synaptically evoked astrocyte calcium signal reveal synaptic information processing by astrocytes. J Neurosci. 2005; 25:2192–203. [PubMed: 15745945]

Perea G, Araque A. Synaptic information processing by astrocytes. J Physiol Paris. 2006; 99:92–7. [PubMed: 16442272]

Perea G, Navarrete M, Araque A. Tripartite synapses: astrocytes process and control synaptic information. Trends Neurosci. 2009; 32:421–31. [PubMed: 19615761]

Peters, A.; Palay, S.; Webster, H. The fine structure of the nervous system. 3rd ed.. Oxford University Press; New York: 1991.

Reichenbach A, Derouiche A, Kirchhoff F. Morphology and dynamics of perisynaptic glia. Brain Res Rev. 2010; 63:11–25. [PubMed: 20176054]

Rogan MT, Leon KS, Perez DL, Kandel ER. Distinct neural signatures for safety and danger in the amygdala and striatum of the mouse. Neuron. 2005; 46:309–320. [PubMed: 15848808]

Sah P, Westbrook RF, Luthi A. Fear conditioning and long-term potentiation in the amygdala: what really is the connection? Ann N Y Acad Sci. 2008; 1129:88–95. [PubMed: 18591471]

Schafe GE, LeDoux JE. Memory Consolidation of Auditory Pavlovian Fear Conditioning Requires Protein Synthesis and Protein Kinase A in the Amygdala. J Neurosci. 2000; 20:RC96. [PubMed: 10974093]

Segal, MM.; Baughman, RW.; Jones, KA.; Huettner, JE. Mass cultures and microislands of neurons from postnatal rat brain. In: Banker, G.; Goslin, K., editors. Culturing Nerve Cells. MIT Press; Cambridge, MA: 1998. p. 339-70.

Spacek J. Three-dimensional analysis of dendritic spines. III. Glial sheath. Anat Embryol (Berl). 1985a; 171:245–52. [PubMed: 3985373]

Spacek J. Three-dimensional analysis of dendritic spines. II. Spine apparatus and other cytoplasmic components. Anat Embryol (Berl). 1985b; 171:235–243. [PubMed: 3985372]

Stehberg J, Moraga-Amaro R, Salazar C, Becerra A, Echeverría C, Orellana JA, Bultynck G, Ponsaerts R, Leybaert L, Simon F, et al. Release of gliotransmitters through astroglial connexin 43 hemichannels is necessary for fear memory consolidation in the basolateral amygdala. FASEB J. 2012; 26:3649–57. [PubMed: 22665389]

Steward O, Levy WB. Preferential localization of polyribosomes under the base of dendritic spines in granule cells of the dentate gyrus. J Neurosci. 1982; 2:284–291. [PubMed: 7062109]

Sutton MA, Schuman EM. Dendritic protein synthesis, synaptic plasticity, and memory. Cell. 2006; 127:49–58. [PubMed: 17018276]

Suzuki A, Stern SA, Bozdagi O, Huntley GW, Walker RH, Magistretti PJ, Alberini CM. Astrocyte-neuron lactate transport is required for long-term memory formation. Cell. 2011; 144:810–23. [PubMed: 21376239]

Theodosis DT, Poulain DA, Oliet SHR. Activity-dependent structural and functional plasticity of astrocyte-neuron interactions. Physiol Rev. 2008; 88:983–1008. [PubMed: 18626065]

Todd K, Serrano A, Lacaille J, Robitaille R. Glial cells in synaptic plasticity. J Physiol Paris. 2006; 99:75–83. [PubMed: 16446078]

Ventura R, Harris K. Three-dimensional relationships between hippocampal synapses and astrocytes. J Neurosci. 1999; 19:6897–906. [PubMed: 10436047]

Verbich D, Prenosil GA, Chang PK-Y, Murai KK, McKinney RA. Glial glutamate transport modulates dendritic spine head protrusions in the hippocampus. Glia. 2012; 60:1067–77. [PubMed: 22488940]

Wang DD, Bordey A. The astrocyte odyssey. Prog Neurobiol. 2008; 86:342–67. [PubMed: 18948166]

Witcher M, Kirov S, Harris K. Plasticity of perisynaptic astroglia during synaptogenesis in the mature rat hippocampus. Glia. 2007; 55:13–23. [PubMed: 17001633]

Xu-Friedman MA, Harris KM, Regehr WG. Three-dimensional comparison of ultrastructural characteristics at depressing and facilitating synapses onto cerebellar Purkinje cells. J Neurosci. 2001; 21:6666–72. [PubMed: 11517256]

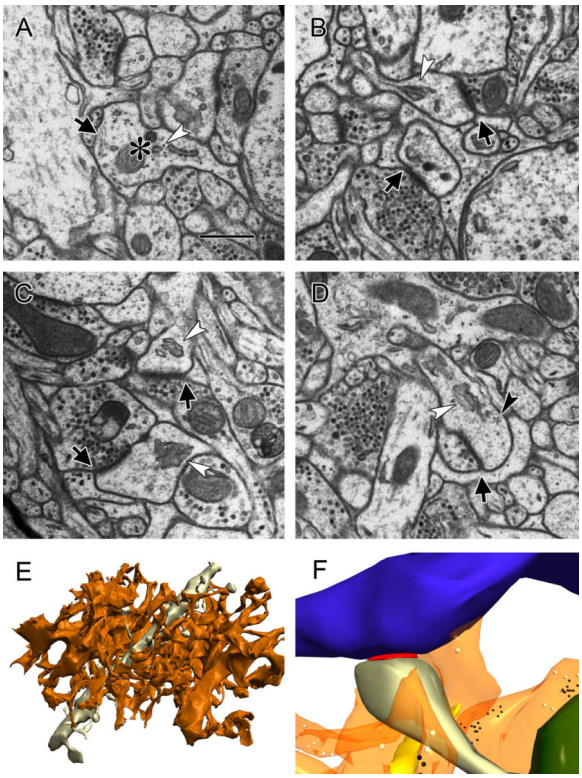

Figure 1.

Astrocytes in the rat lateral amygdala. A) Electron micrograph of an astrocytic process (asterisk) containing distinctive filamentous structures (arrow) and glycogen granules (i.e. arrowhead). scale=500nm B-D) Contact between astrocytic processes and the synaptic cleft (arrows) at spines with a spine apparatus (white arrowheads) and polyribosomes (black arrowhead in D). E) Three dimensional reconstruction of the processes of a single astrocyte contained in one 930μm^3 tissue volume (orange), with a 10.25μm dendritic segment (gray). F) Reconstruction of a tripartite synapse. Blue: axon; gray: dendrite; orange: astrocyte; red: synaptic cleft; green: mitochondria; yellow: smooth endoplasmic reticulum; black: ribosomes; white: glycogen granules.

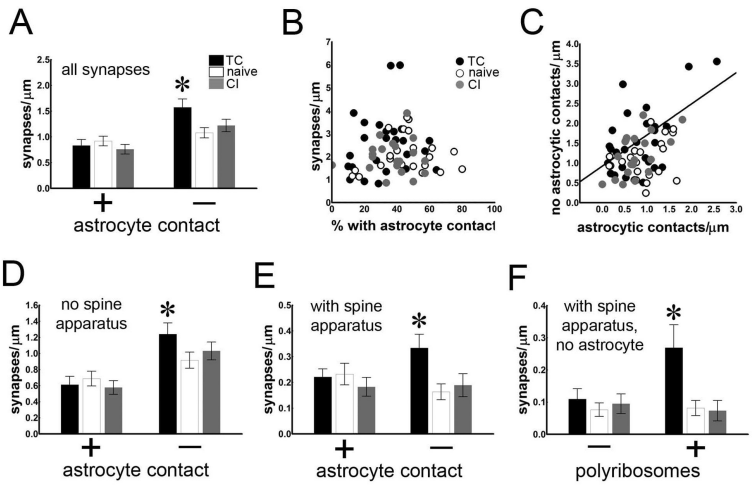

Figure 2.

Density of astrocytic contacts at spine synapses along dendrites. A) Density of synapses with and without astrocytic contacts (*p<0.01). B) Synapse density versus percentage of synapses with astrocytic contacts. C) Density of synapses with versus without astrocytic contacts per micron length of dendrite (TC group R^2=0.31, p<0.004). D) Density of synapses without an associated spine apparatus with and without astrocytic contacts (*p<0.05). E) Density of synapses with an associated spine apparatus with and without astrocytic contacts (*p<0.007). F) Density of synapses with an associated spine apparatus and no astrocytic contact, with and without polyribosomes (*p<0.004).

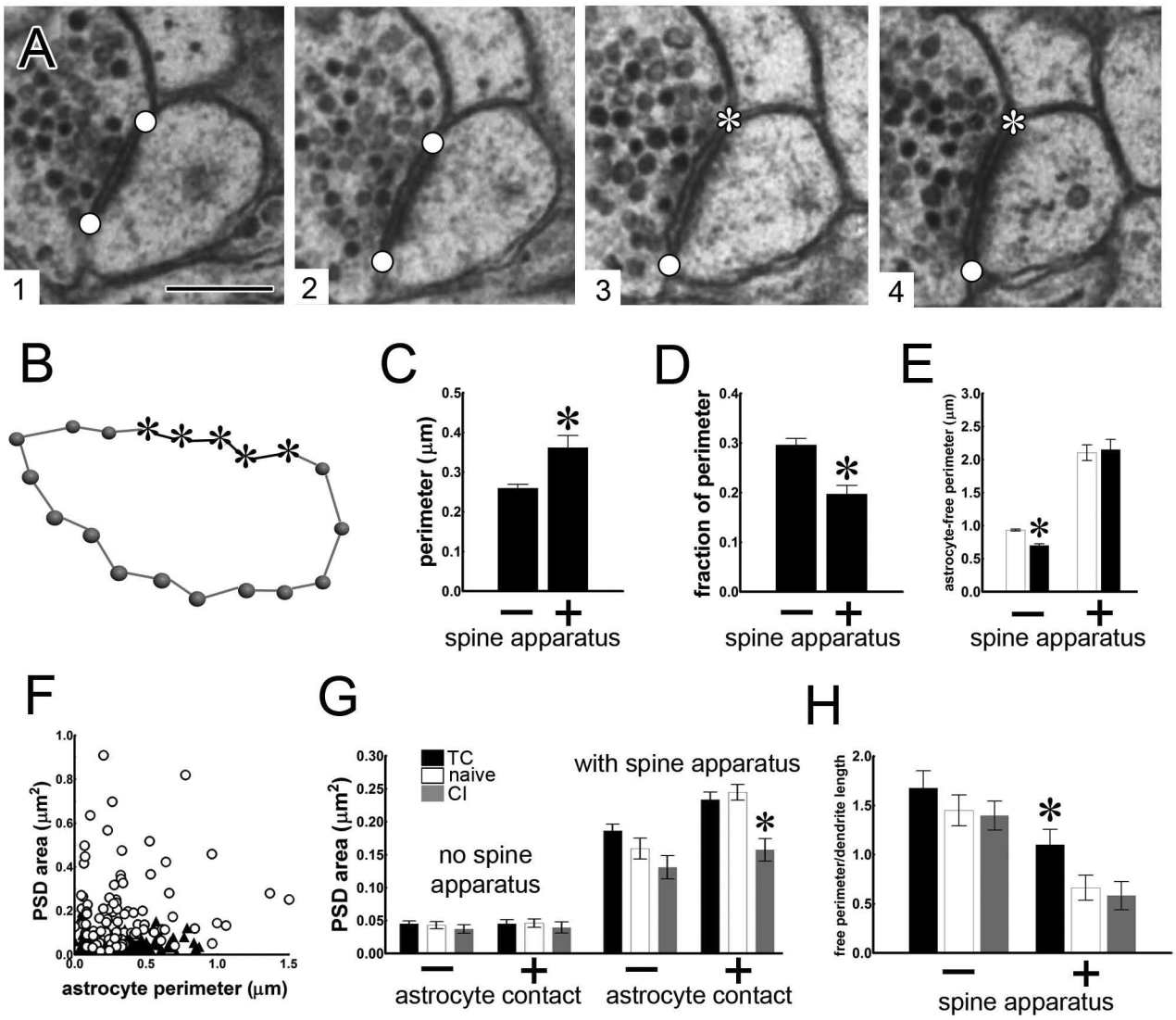

Figure 3.

Stability of the astrocytic contact perimeter. A) Four serial sections of a synapse showing points along which the perimeter of the synaptic cleft was measured. Asterisks mark points with an astrocytic process contact with the synaptic cleft and circles mark points without astrocytic contact. scale=250nm B) Complete point-to-point reconstruction of the entire perimeter of the synaptic cleft in (A). The asterisks indicate contact with an astrocyte, and the black line between them is the length of the perimeter in contact with astrocyte. C) Length of PSD perimeter covered by astrocyte at spines with and without a spine apparatus (SA; *p<0.001). D) Fraction of synapse perimeter covered by astrocyte (*p<0.002). E) Length of astrocyte-free PSD perimeter at synapses without (white bars) and with astrocytic contacts (black bars). Synapses with and without a spine apparatus were different from each other (*p<0.0001; bars not shown for clarity). F) Astrocyte-covered PSD perimeter versus PSD area (R^2=0.02) at SA-free (triangles) and SA synapses (circles). G) PSD area by training group, SA, and astrocytic contact (*p<0.00001, CI versus naive). SA synapses with astrocytic contact are larger in the TC (p<0.003) and naïve (p<0.00001) groups than those without (bars not shown for clarity). H) Length of astrocyte-free asymmetric synapse perimeter per length of dendrite (*p<0.02).

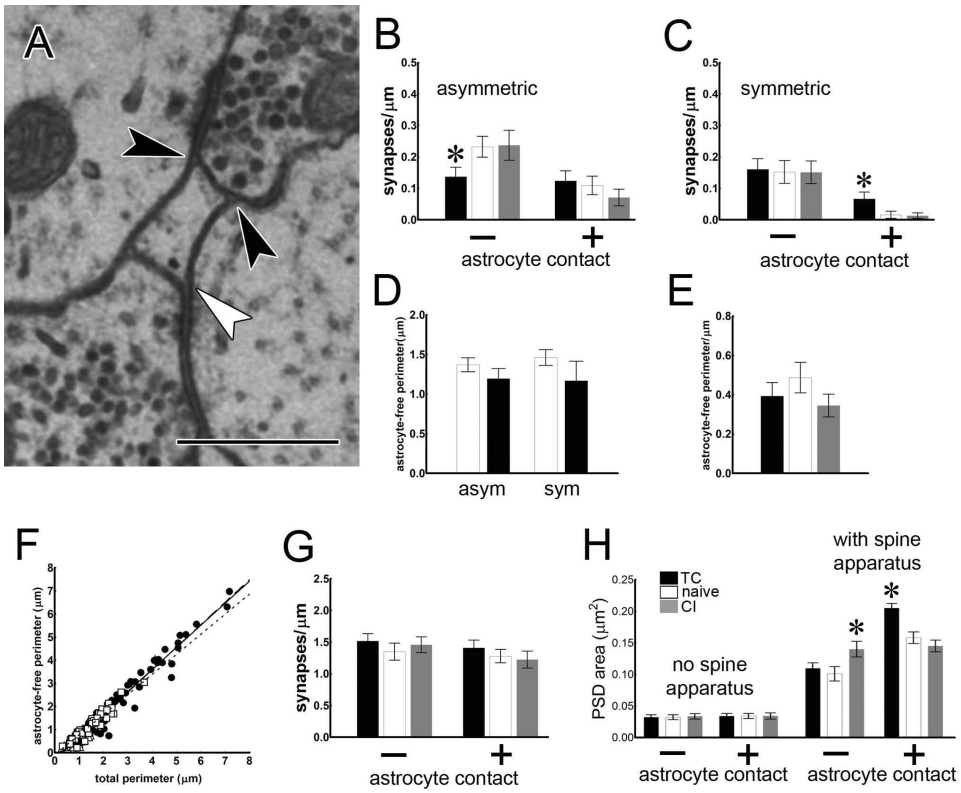

Figure 4.

Shaft synapses. A) Electron micrograph of an astrocytic process contacting two asymmetric shaft synapses (black arrowheads) and a symmetric shaft synapse (white arrowhead). scale=500nm B) Density of asymmetric shaft synapses with and without astrocytic contacts (*p<0.05). C) Density of symmetric shaft synapses with and without astrocytic contacts (*p<0.03). D) Length of astrocyte-free perimeter on shaft synapses without (white bars) and with astrocytic contacts (black bars). E) Length of astrocyte-free perimeter of asymmetric shaft synapses per length of dendrite. F) Length of total PSD perimeter versus astrocyte-free perimeter (SA-free R^2=0.82, triangles, dashed line, SA R^2=0.95 circles, solid line, shaft R^2=0.90, squares, dotted line). G) Density of synapses with and without astrocytic contacts 24 hours after training. H) PSD area of synapses with and without SA and astrocytic contacts 24 hours after training. (*p<0.003).